Croatian Society for Materials Protection

Metalurgija/Metallurgy

Vol. 66 No. 1 / 2027

Study on Creep Resistance and Feasibility of Titanium Alloy Ti60 for Organ Pipe Tubes

Wen Sun [1,*]

https://doi.org/10.64486/m.66.1.10

[1] Harbin University, Harbin City, Heilongjiang Province, China
* Correspondence: sunwen@lsu.edu.gn; Tel.: +8613136688185

Type of the Paper: Article
Received: January 5, 2026
Accepted: June 23, 2026

Abstract: Pipe organs rely on the long-term dimensional stability of metal tubes to maintain accurate intonation, while traditional tin-lead alloy tubes are susceptible to room-temperature creep, which may lead to irreversible deformation and pitch drift. This theoretical feasibility study (without new experimental testing or acoustic validation) explores the potential of the newly developed Ti60 high-temperature titanium alloy as an organ pipe material from the perspective of creep resistance. The analysis is based on published high-temperature creep data and physically constrained mathematical extrapolation. Published creep data for Ti60 alloy at 550 °C indicate a typical three-stage creep behavior, including primary, secondary, and tertiary creep stages, with a minimum steady-state creep rate of 0.04 h^{-1} under the reported test conditions. Based on the creep deformation mechanism dominated by dislocation motion and on the Arrhenius relationship describing the temperature dependence of creep rate, the study suggests that Ti60 may exhibit extremely low creep deformation under low-stress room-temperature conditions. It should be emphasized that this conclusion is based solely on theoretical extrapolation and does not represent experimental verification of actual service performance. Using an established creep constitutive model, mathematical extrapolation, and mechanistic analysis of high-temperature creep behavior, this work provides a preliminary theoretical assessment of the feasibility of Ti60 as an alternative organ pipe material in terms of creep resistance. The results suggest a potential direction for future research aimed at reducing long-term dimensional deformation caused by room-temperature creep and supporting the preservation of pipe organ cultural heritage.

Keywords: Ti60 alloy; organ pipe tube; creep property; creep constitutive model; room-temperature creep extrapolation

1. Introduction

The acoustic performance and long-term stability of a pipe organ fundamentally depend on the physical integrity of its thousands of metal tubes. As core sound-generating components, organ tubes require strict coupling of acoustic properties and mechanical stability: they must maintain consistent geometric dimensions, wall thickness, and surface quality during decades of service to ensure stable air vibration characteristics and fixed pitch. Material creep—an irreversible plastic deformation caused by long-term exposure to static stress—is a key technical challenge in this field. At room temperature, even low-stress environments can induce slow plastic flow in materials, leading to micro-scale changes in the geometric dimensions of the tubes. Existing studies have confirmed that this dimensional deformation is the core material factor leading to the alteration of air vibration characteristics and subsequent irreversible pitch drift, which deviates significantly from the original tuning. Over time, such material creep renders the organ's intonation uncorrectable, imposing enormous maintenance burdens on historical instruments [1].

Meanwhile, the traditional tin-lead alloy tubes face increasingly stringent environmental protection constraints due to their toxicity, further limiting their application. Although the industry retains affection for the traditional timbre of these alloys, developing alternative materials with excellent long-term stability and environmental compatibility has become an urgent priority. Adding other alloying elements to tin-lead alloys to enhance performance fails to meet the required stability; high-entropy alloys, while promising, are costly and difficult to tune to match traditional timbres, making them impractical for large-scale use. These limitations have driven the exploration of new materials in the field of organ tube manufacturing [1].

Recent advances in high-temperature alloy technology have opened new possibilities for addressing this challenge. The high-temperature alloy Ti60 (Ti-5.8Al-4Sn-4Zr-2Mo-1.5Ta-0.8Si-0.06C) was designed for extreme service environments [3-6]. Through precise microstructural control—including regulation of phase structure and carbide dispersion—it maintains stable creep and microstructural properties above 550 °C [7-9]. Published systematic studies in the existing literature have confirmed that its creep behavior follows the classic three-stage creep pattern, and a complete set of high-temperature creep performance data and corresponding creep constitutive models have been established, which provides a reliable data basis for the theoretical extrapolation in this study. The high-temperature creep resistance of Ti60 originates from its stable α-phase matrix and high activation energy for dislocation motion; according to the classic creep theory, the steady-state creep rate of metals follows the Arrhenius relationship with temperature, which means that the high activation energy for creep deformation will lead to an extremely low creep rate at room temperature, even under low stress. This intrinsic characteristic provides a physical basis for the theoretical extrapolation of its long-term creep deformation at room temperature and low stress, which is the core performance requirement for the long-term dimensional stability of organ tubes. This raises a critical hypothesis for this theoretical study: the microstructural features that enable excellent high-temperature creep resistance of Ti60 alloy may confer extremely low creep deformation rate in the low-temperature, low-stress service environment of organ tubes. If its room-temperature creep rate is quantitatively lower than that of traditional tin-lead alloys through theoretical extrapolation, it may provide a potential theoretical research direction for alleviating the long-term dimensional deformation of organ tubes caused by room-temperature creep [10].

It is critical to explicitly clarify the research scope and limitations at the outset: this study only focuses on the theoretical assessment of creep resistance of Ti60 alloy, and conducts a preliminary theoretical feasibility analysis of its application in organ pipe tubes exclusively from the perspective of creep-induced dimensional deformation. This study does not involve any acoustic performance testing, timbre tuning and optimization, or experimental verification of pitch stability, and all conclusions related to room-temperature performance are theoretical extrapolation results based on published high-temperature creep data, with non-negligible limitations. The application to organ pipe tubes is selected as a representative case to conduct a preliminary theoretical assessment of the material's long-term creep resistance and application potential in low-stress room-temperature service scenarios. This theoretical feasibility study adopts a "published data analysis-theoretical modeling-physically constrained extrapolation" research approach: instead of conducting new material tests, it systematically analyzes publicly available Ti60 alloy high-temperature creep data (including complete creep curves and stress-strain characteristics under different stress levels at 550 °C) to establish a unified creep constitutive model. This study focuses on verifying three core theoretical propositions: first, whether the high-temperature creep resistance mechanism of Ti60 alloy has the physical basis for theoretical extrapolation to room-temperature low-stress service scenarios; second, whether the theoretically extrapolated room-temperature creep deformation of the material may be sufficient to meet the long-term dimensional stability requirements of organ pipe tubes via mathematical modeling; third, the engineering feasibility of processing Ti60 alloy into organ pipe tubes under modern precision manufacturing technologies.

 https://doi.org/10.64486/m.66.1.10

The innovation of this study lies in its theoretical and feasibility-oriented methodology: it provides preliminary theoretical reference for solving engineering-level problems in traditional craftsmanship, offering a new solution for preserving classic traditional instruments. Based on the extrapolation results with explicit limitations, this study preliminarily infers that Ti60, as a new alternative material option, may provide a "materials science-driven" innovative research path for organ tube manufacturing. This could enable the long-term preservation and innovative development of the pipe organ as a cultural heritage, and serve as a reference for applying advanced engineering materials to solve technical bottlenecks in other traditional craftsmanship fields.

2. Analysis of Material Performance Basis and Experimental Methods

2.1. Experimental Materials and Standard Specimens

All material performance data and specimen parameters in this study are derived from publicly available literature; no new experimental tests were carried out. The nominal chemical composition of the Ti60 alloy analyzed in this study is Ti-5.8Al-4Sn-4Zr-0.7Nb-1.5Ta-0.4Si-0.06C, which belongs to the near alpha high-temperature titanium alloy. According to the published studies [12-13], the specimens had a plate-like geometry, and their dimensions were designed in accordance with the reported testing standards. Specifically, the reported specimens had a gauge section width ranging from approximately 15.00 mm to 15.20 mm and a thickness ranging from 1.50 mm to 1.54 mm; this dimensional design ensures highly uniform stress distribution in the gauge section during axial loading, thereby obtaining creep data that truly reflects the material's intrinsic properties. The geometric morphology of the specimen (as shown in Figure 1) is a primary prerequisite for ensuring the comparability and reliability of all subsequent performance data. [14-17].

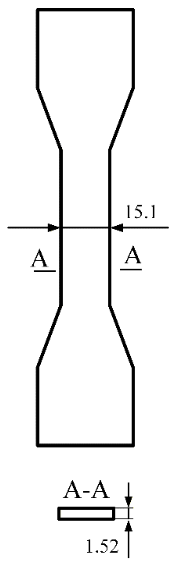

Figure 1. Standardized Geometric Morphology of the Specimen

Figure 2. Instron-5980 Universal Testing Machine

2.2 Experimental Equipment and High-Temperature Environment Control

According to the original studies, all creep and creep-fatigue interaction tests were conducted on an Instron-5980 universal testing machine. As shown in Figure 2, this machine is equipped with a high-rigidity frame and a precise closed-loop control system, enabling long-term stable control and high-precision measurement of load and displacement—it is a key device for acquiring reliable long-duration creep data.

Tests were performed in a constant high-temperature environment of 550 °C, with a temperature control accuracy of ±2 °C. Prior to testing, the specimen was held at the target temperature for a sufficient duration to

https://doi.org/10.64486/m.66.1.10

ensure uniformity and stability of the overall temperature field, thereby eliminating the influence of thermal gradients on initial strain and early creep behavior.

The combination of the high-temperature environment chamber and a high-precision high-temperature extensometer enables real-time, continuous monitoring of micro-strain in the specimen under harsh thermal conditions, providing technical support for capturing complete creep curves [18].

2.3 Loading Protocol: Creep-Fatigue Interaction Spectrum

To simulate the cumulative damage behavior of engineering components under long-term alternating load and static load service conditions, a carefully designed creep-fatigue interaction load spectrum (loading waveform shown in Figure 3) was adopted in the original literature tests. This spectrum consists of periodically applied alternating fatigue load blocks, followed by constant creep hold blocks [19].

In the tests, the fatigue load segment was controlled by stress: the maximum stress (σ_{max}) was fixed at 450 MPa, the stress ratio R (ratio of minimum stress to maximum stress) was 0.1, and the loading waveform was a sine wave. Each load block contained 64 fatigue cycles [20].

In the original study, the stress level (σ_{creep}) during the creep hold stage was systematically varied, with multiple stress levels ranging from 345 MPa to 450 MPa being selected. By keeping the fatigue loading parameters constant and varying only the creep stress, the influence of creep stress on damage accumulation and fatigue-creep life could be evaluated. Each complete fatigue-creep loading sequence constituted one loading block, and multiple blocks were applied consecutively during the tests.

Two termination conditions were set for the tests:

1) Reaching the preset total test duration (e.g., 50 hours or 100 hours);
2) Real-time monitoring via the high-temperature extensometer showing that the axial total strain of the specimen reaches 1.0 %.

The latter serves as a clear engineering failure criterion, used to determine whether the material has undergone harmful plastic deformation under specific loading conditions, thereby providing a quantitative basis for evaluating the "threshold" effect of different creep stress levels.

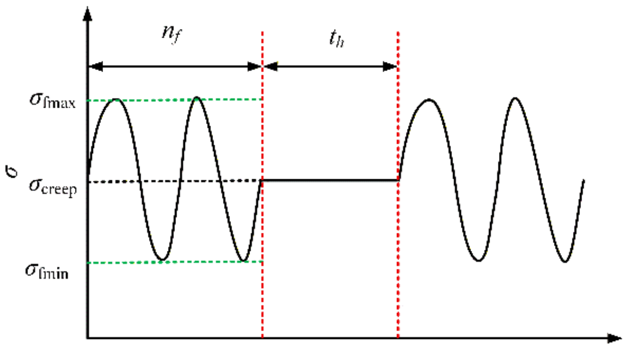

Figure 3. Schematic Diagram of Loading Waveform

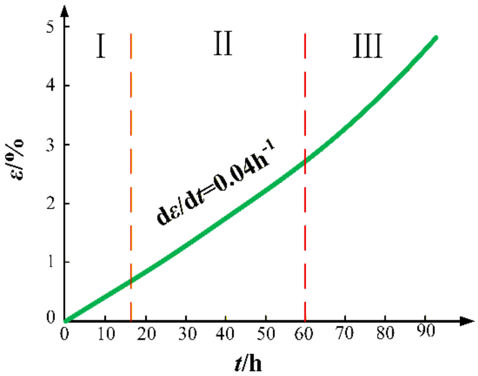

Figure 4. Strain-Time Curve at 550 °C, σ_{max}=450 MPa, σ_{creep}=450 MPa

3. Analysis of Test Results and Derivation of Constitutive Model

3.1 Analysis of Creep Behavior Characteristics

A typical strain-time curve obtained from the tests (Figure 4) shows that the Ti60 alloy exhibits the classic three-stage creep behavior at 550 °C under a creep stress (σ_{creep}) of 450 MPa:

1) Stage I (Region I): Primary transient creep, where the strain rate decreases rapidly;
2) Stage II (Region II): Steady-state creep, where the strain rate remains constant (0.04 h^{-1} in the curve). This stage lasts for a long duration, accounting for the main portion of the creep life;
3) Stage III (Region III): Accelerated creep, where the strain rate increases rapidly until fracture.

 https://doi.org/10.64486/m.66.1.10

Creep curves under different stress levels are presented in Figures 5 and 6. The analysis indicates that:

1) When the creep stress is ≤ 390 MPa, the steady-state creep rate remains nearly consistent;
2) When the creep stress exceeds 405 MPa, the steady-state creep rate increases significantly with rising stress.

This suggests the presence of a critical stress range between 390 MPa and 405 MPa that may influence the creep behavior of the alloy, providing a theoretical basis for the subsequent feasibility analysis.

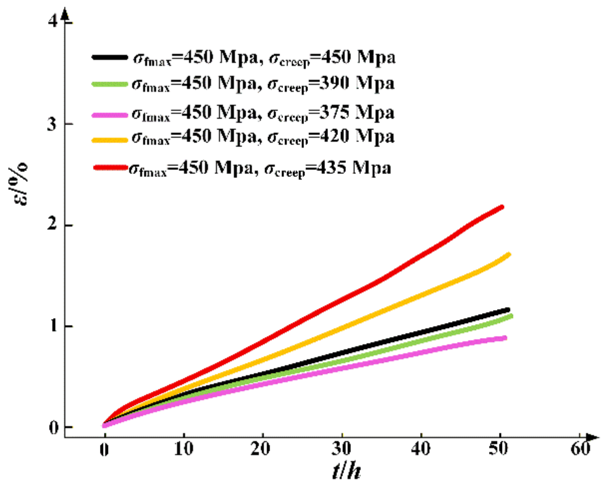

Figure 5. Creep-Fatigue Test Strain-Time Curve (Test Duration: 50 h)

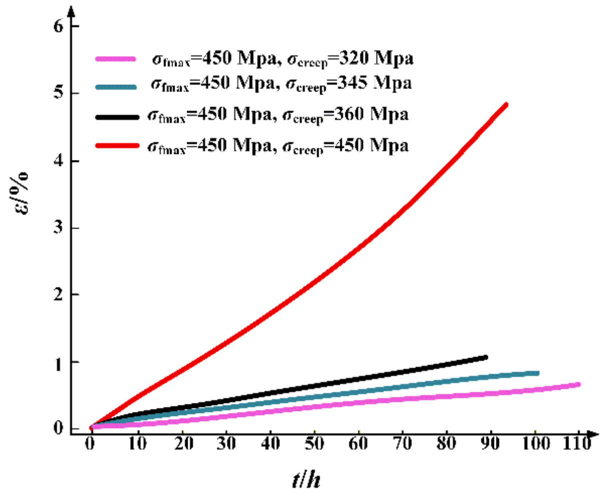

Figure 6. Creep-Fatigue Test Strain-Time Curve (Test Duration: 100 h)

3.2 Derivation of the Constitutive Model

To quantitatively characterize the creep behavior of the Ti60 alloy and provide a theoretical model for subsequent room-temperature creep extrapolation, a corresponding creep constitutive model was established based on the published test data. A creep constitutive equation describes the relationship between a material's creep deformation and loading parameters (temperature, time, stress, etc.). For the steady-state creep stage, which is the core stage affecting the long-term dimensional stability of materials, the most widely used model is the Norton power law, which is coupled with the Arrhenius equation to describe the temperature dependence of creep rate, expressed as:

$$\dot{\varepsilon}_{ss} = A \cdot \sigma_{creep}^{n} e^{\left(-\frac{Q}{RT}\right)} \quad (1)$$

Where:

$\dot{\varepsilon}_{ss}$ = steady-state creep rate
A = temperature-dependent material constant
σ_{creep} = creep stress
n = stress exponent
Q = activation energy for creep deformation
R = universal gas constant
T = absolute temperature.

This equation provides the physical basis for extrapolating high-temperature creep data to room-temperature conditions. The extrapolation is based on the assumptions that the dominant creep deformation mechanism remains unchanged and that the activation energy Q and stress exponent n do not vary significantly with temperature. Under these assumptions, the steady-state creep rate at room temperature can be theoretically estimated from the available high-temperature creep data.

https://doi.org/10.64486/m.66.1.10

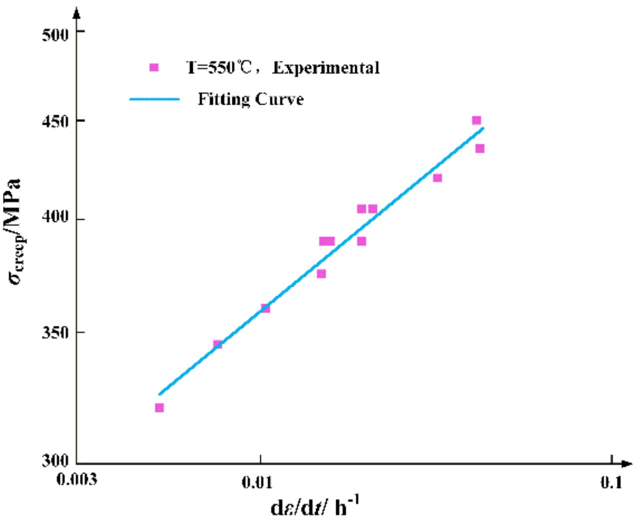

Figure 7. Creep-Fatigue Test Strain-Time Curve (Test Duration: 50 h)

Figure 7 shows the relationship between the steady-state creep rate and creep stress of Ti60 alloy at 550 °C plotted on a double-logarithmic coordinate system. The data points exhibit a good linear distribution, supporting the applicability of the Norton law under the test conditions. To determine parameters A and n at 550 °C, the steady-state creep rate was extracted from strain-time curves under different σ_{creep} values, and linear regression fitting was performed on the data. The fitting result is:

$$\sigma_{creep} = 715.8631 \cdot (\dot{\varepsilon}_{ss})^{0.14995} \quad (2)$$

The corresponding stress exponent n obtained by inversion is 6.67, which is consistent with the typical stress exponent value of a dislocation glide and climb controlled creep mechanism in titanium alloys, supporting the interpretation that the creep deformation of Ti60 alloy at 550 °C is dominated by dislocation motion. This model quantifies the strong dependence of the steady-state creep rate on the driving stress, which is consistent with a creep deformation mechanism dominated by dislocation motion, and serves as a theoretical basis for estimating the long-term deformation rate of the material through theoretical extrapolation.

The Norton law only describes the strain rate in the steady-state stage. To characterize the relationship between the total accumulated creep strain ε_c (from loading initiation to the end of the steady-state stage) and time t as well as stress σ_{creep}, a more comprehensive constitutive model is required. Based on the phenomenological method, a widely used power-law expression was adopted:

$$\varepsilon_c = B \cdot t^m \cdot \sigma_{creep}^p \quad (3)$$

Where:

B, m, p = material parameters to be determined.

To identify these parameters, creep test curves with σ_{creep} values of 360 MPa, 390 MPa, and 450 MPa were selected for fitting. The parameter values obtained from the fitting results are listed in Table 1 below.

Table 1. Material Parameters Under Different Creep Stresses Fitted by the Power-Law Model

σ_{creep}/ MPa	m	p
360	0.856	-0.710
390	0.790	-0.502
450	1.283	-0.645

Analysis of Table 1 data reveals that parameter p shows no obvious trend with stress variation, and its average value is approximately -0.619. However, parameter m exhibits a clear positive correlation with σ_{creep}. To establish a quantitative relationship between m and σ_{creep}, p was fixed at its average value (-0.619), and the test data were refitted. The fitting results indicate a good linear relationship between m and σ_{creep}, yielding the linear fitting equation:

$$m = 0.00552 \cdot \sigma_{creep} - 1.219 \quad (4)$$

Substituting the relationship between m and σ_{creep}, along with the average value of p, into the initial power-law model, the unified full-stage creep constitutive equation for Ti60 alloy at 550 °C is obtained:

$$\varepsilon\_c \ (\sigma\_creep, t) = B \cdot t\hat{}(0.00552\sigma\_creep - 1.219) \cdot \sigma\_creep\hat{}(-0.619) \quad (5)$$

Where:
B = normalized constant.

A notable feature of this equation is the expression of the exponent m (the time term) as a linear function of stress, which suggests that the rate of creep damage accumulation is not only time-dependent, but that its evolution may also be influenced by the stress level.

Further derivation of Equation (5) extends the model to a more general form combined with the Arrhenius temperature relationship, which can be used for theoretical extrapolation of creep deformation at different temperatures:

$$\varepsilon_c(\sigma_{creep}, t) = C \cdot t^{k_1\sigma_{creep} - k_2} \cdot \sigma_{creep}^{k_3} \quad (6)$$

Where, C, k_1, k_2, k_3 are material constants calibrated via test data at a specific temperature. For the Ti60 alloy in this study (at 550 °C), k_1 = 0.00552, k_2 = −1.219, k_3 = −0.619.

This model integrates the experimental observations: it not only incorporates the stress-strain rate power-law relationship for the steady-state stage, but also describes the nonlinear time-dependent evolution of creep strain and its stress dependence via $t^{0.00552\sigma_{creep} - 1.219}$. More importantly, it incorporates the temperature dependence of creep deformation, thereby providing a theoretical framework for the subsequent extrapolation of room-temperature creep behavior of Ti60 alloy.

4. Theoretical Feasibility Assessment Based on Creep Constitutive Model

4.1 Theoretical Extrapolation of Room-Temperature Creep Deformation and Preliminary Assessment of Dimensional Stability Potential

The high-temperature creep resistance of Ti60 alloy at 550 °C provides a basis for the theoretical extrapolation of its creep performance under room-temperature conditions; however, it cannot be regarded as direct evidence of its performance in room-temperature organ pipe applications. All room-temperature performance inferences presented in this section are based on theoretical extrapolation under explicit assumptions and are subject to non-negligible limitations. Therefore, they should not be considered proof of the material's actual long-term dimensional stability in organ pipe service conditions.

4.1.1 Explicit Assumptions for Theoretical Extrapolation

To ensure the physical rationality of the extrapolation, the following strict assumptions are clearly defined for the extrapolation from 550 °C high-temperature data to room-temperature (25 °C) low-stress conditions:

1) The creep deformation mechanism of Ti60 alloy remains dominated by dislocation glide and climb within the temperature range from 550 °C to room temperature, and the stress exponent n and creep activation energy Q do not vary significantly over the considered temperature range.
2) Power law applicability assumption: The Norton power law coupled with the Arrhenius equation is still applicable to the low-stress room-temperature service conditions of organ pipe tubes.
3) Stress state assumption: The organ pipe tube is in a stable low static stress state during service, and the stress level is much lower than the yield strength of Ti60 alloy at room temperature.
4) Environmental stability assumption: The influence of ambient humidity, corrosion, material aging and other factors in the actual service environment on the creep behavior of the material is not considered in the extrapolation model.

 https://doi.org/10.64486/m.66.1.10

4.1.2 Theoretical Extrapolation Calculation and Preliminary Assessment

The extrapolation analysis presented in this section is based on the explicit assumptions defined in the previous section and on the temperature-dependent creep constitutive model established in this study. All results represent theoretical inferences only and do not constitute experimental verification of actual service performance.

Based on classical creep theory, which relates creep behavior to temperature and stress conditions, and considering the high-temperature creep characteristics reported for Ti60 alloy, a preliminary theoretical assessment of its creep behavior under room-temperature low-stress conditions was performed. The high-temperature creep resistance of Ti60 alloy has been attributed in the literature to its stable microstructure, the strengthening effect of dispersed phases, and the relatively high activation energy associated with creep deformation. Under the assumptions adopted in this study, these characteristics may contribute to a low tendency for creep deformation under room-temperature service conditions.

Previous studies have shown that room-temperature creep of traditional tin-lead alloys can contribute to long-term dimensional instability of organ pipes. Within the theoretical framework adopted in this study, Ti60 alloy is expected to exhibit greater resistance to creep deformation than traditional tin-lead alloys under comparable low-stress conditions. Consequently, Ti60 alloy may have the potential to contribute to improved long-term dimensional stability of organ pipe tubes.

It should be emphasized that the above conclusions are based solely on theoretical extrapolation of published high-temperature creep data and are valid only within the assumptions defined in this study. They should therefore be regarded as preliminary theoretical estimates rather than confirmation of actual service performance.

4.1.3 Clear Limitations of Extrapolation Results

The extrapolation results have clear and non-negligible limitations, which must be emphasized:

1) Lack of direct experimental verification: There is no direct long-term creep test data of Ti60 alloy at room temperature to verify the prediction accuracy of the extrapolation model;
2) Unconsidered environmental factors: Factors such as ambient humidity, minor corrosion, and material aging in the actual service environment may affect the creep behavior of the material, but are not considered in the current extrapolation model;
3) Uncertainty of creep mechanism: The creep mechanism of the material may change at room temperature and low stress, which will lead to the deviation of the extrapolation results from the actual situation;
4) No acoustic performance validation: This study does not involve any acoustic performance testing or timbre matching research of Ti60 alloy organ pipe tubes, and cannot prove the acoustic acceptability of the material for organ pipe applications.

All the above room-temperature performance inferences are only preliminary theoretical estimates based on high-temperature data extrapolation, and cannot be used as direct proof of the material's actual long-term dimensional stability or acoustic applicability in organ pipe service scenarios.

4.2 Theoretical Assessment of Engineering Processing Feasibility

Although Ti60 alloy is known to present certain machining challenges, published studies indicate that advanced precision manufacturing technologies are available for processing titanium alloys with high dimensional accuracy. Techniques such as five-axis CNC machining, wire electrical discharge machining, and metal additive manufacturing have been successfully applied to the fabrication of complex titanium alloy components [13,19].

Based on the capabilities of these existing manufacturing technologies, the production of Ti60 alloy organ pipe components may be technically feasible. However, the actual manufacturability of thin-walled Ti60 organ pipes, including forming, joining, dimensional control, surface quality, and production costs, has not been

https://doi.org/10.64486/m.66.1.10

investigated in this study and remains to be experimentally verified. Therefore, the engineering feasibility discussed here should be regarded as a preliminary theoretical assessment based on existing manufacturing technologies rather than as confirmation of practical manufacturing capability for organ pipe applications.

4.3 Comprehensive Theoretical Advantages and Gradual Application Research Path

Based on the theoretical analysis presented in this study, Ti60 alloy may represent a promising candidate for further investigation as an organ pipe material. In addition to its potential advantages in creep resistance, the alloy may offer benefits associated with its lead-free composition, corrosion resistance, and environmental durability. However, these potential advantages are inferred from published material properties and theoretical extrapolation and have not yet been experimentally verified for organ pipe applications.

Therefore, further research is required, including long-term room-temperature creep testing, acoustic characterization, and evaluation of manufacturing feasibility before any practical application can be considered.

5. Conclusions

This study presents a theoretical feasibility assessment of the potential use of Ti60 near-α high-temperature titanium alloy as an alternative material for organ pipe tubes from the perspective of creep resistance. Based on the analysis of published high-temperature creep data and physically constrained extrapolation, the following conclusions can be drawn:

1. Ti60 alloy exhibits high creep resistance at 550 °C, characterized by a low steady-state creep rate and a prolonged steady-state creep stage. A temperature-dependent creep constitutive model coupled with the Arrhenius equation was employed to provide a physically based framework for extrapolating high-temperature creep data to room-temperature conditions.
2. Under the assumptions adopted in this study, theoretical calculations suggest that the steady-state creep rate of Ti60 alloy under room-temperature low-stress conditions may be several orders of magnitude lower than that of traditional tin-lead alloys. These results indicate the potential of Ti60 alloy to provide improved long-term dimensional stability and suggest a possible research direction for mitigating dimensional deformation of organ pipes associated with room-temperature creep.
3. Based on the available literature and the theoretical analysis presented in this study, Ti60 alloy appears to be a promising candidate for further investigation as an alternative organ pipe material. Nevertheless, its practical applicability, manufacturability, acoustic performance, and long-term service behavior remain to be established through experimental validation.

This study has several important limitations. All conclusions regarding the room-temperature performance of Ti60 alloy are based on theoretical extrapolation of published high-temperature creep data and do not constitute experimental verification of actual service performance. Furthermore, acoustic performance, timbre characteristics, and pitch stability of Ti60 organ pipes have not been experimentally evaluated. Consequently, the applicability of Ti60 alloy in organ manufacturing remains to be verified through dedicated experimental studies. In addition, the extrapolated results may differ from actual performance due to possible changes in creep mechanisms and other environmental or service-related factors.

Future research should focus on long-term room-temperature creep testing of Ti60 alloy, experimental validation of the extrapolation model, acoustic characterization of Ti60 organ pipes, and investigation of manufacturing technologies for thin-walled Ti60 organ pipe components.

References

[1] P. Kowol, et al. "Pipe Organ Design Including the Passive Haptic Feedback Technology and Measurement Analysis of Key Displacement, Pressure Force and Sound Organ Pipe." Applied System Innovation vol.7, no.3, pp.37-, 2024, https://doi.org/10.3390/ASI7030037

[2] S. L. Dong, et al. "High temperature tensile creep behavior and microstructure evolution of Ti60 alloy rolled sheet." Materials Today Communications, vol.41, pp.110805-110805, 2024, https://doi.org/10.1016/J.MTCOMM.2024.110805

[3] W. Z. Chen, et al. "The role of grain orientation in NaCl-induced corrosion and stress corrosion cracking of Ti60 alloy at 600 °C." Materials Letters, vol.407, pp.140047-140047, 2026, https://doi.org/10.1016/J.MATLET.2026.140047

[4] C. L. Chen, et al. "Crack nucleation mechanism of Ti60 titanium alloy under ultrasonic fatigue loading at different temperatures." Journal of Physics: Conference Series, vol.2569, no.1, 2023, https://doi.org/10.1088/1742-6596/2569/1/012011

[5] Z. Gong, et al. "Enhanced fracture toughness of Ti60 alloy with lamellar structure obtained by solution-aging treatment." Journal of Materials Science, vol.60, no.33, pp.1-13, 2025, https://doi.org/10.1007/S10853-025-11269-8

[6] S.Z. Jin, et al. "Fatigue damage and life assessment of Ti60 alloy fabricated by laser-directed energy deposition." Welding in the World, vol.69, no.11, pp.1-18, 2025, https://doi.org/10.1007/S40194-025-02124-0

[7] Y. J. Li, et al. "Combustion characteristics and surface damage mechanism of Ti60 alloy under high-speed rubbing." Journal of Materials Science, vol.60, no.27, pp.1-20, 2025, https://doi.org/10.1007/S10853-025-11054-7

[8] Y.X. Wang, et al. "Achieving superior high-temperature performance in Ti60 alloy with dispersed TiC reinforcement via directed energy deposition." Composites Part B, vol.304, pp.112690-112690, 2025, https://doi.org/10.1016/J.COMPOSITESB.2025.112690

[9] T. L. Cai, et al. "Exploring the effects of solution temperature and cooling rate on α phase in a multicomponent titanium alloy: Insights from phase-field simulations." Journal of Alloys and Compounds, vol.1010, pp.177318-177318, 2025, https://doi.org/10.1016/J.JALLCOM.2024.177318

[10] Y.X. Ai, et al. "Near α titanium alloy Ti60 with equiaxed β grain fabricated by laser direct energy deposition assisted with ultrasound." Materials & Design, vol.252, pp.113768-113768, 2025, https://doi.org/10.1016/J.MATDES.2025.113768

[11] K.P. Han, et al. "Evolution and anti-fatigue mechanism of surface characteristics of Ti60 alloy induced by ball burnishing and shot peening during tensile-compression fatigue." Engineering Failure Analysis, vol.159, pp.108136-, 2024, https://doi.org/10.1016/J.ENGFAILANAL.2024.108136

[12] T. Xu, et al. "Effect of post-weld heat treatment on microstructure and mechanical properties of linear friction welded Ti60/Ti17 dissimilar titanium alloy joint." Materials Characterization, vol.229, pp.115492-115492, 2025, https://doi.org/10.1016/J.MATCHAR.2025.115492

[13] Z. Gong, et al. "High-Temperature Three-Point Bending Property of Ti60 Alloy Rolled Sheet Before and After Vacuum Solution Aging Treatment." Advanced Engineering Materials, vol.27, no.10, pp.2403028-2403028, 2025, https://doi.org/10.1002/ADEM.202403028

[14] Z. Gong, et al. "Effect of solution-aging treatment on microstructure and high temperature fracture toughness of Ti60 alloy rolled sheet." Materials Characterization, vol.221, pp.114771-114771, 2025, https://doi.org/10.1016/J.MATCHAR.2025.114771

[15] Y. Li, et al." Superplastic deformation and macrozone behavior of the Ti60 high-temperature titanium alloy." Journal of Alloys and Compounds, vol.1012, pp.178382-178382, 2025, https://doi.org/10.1016/J.JALLCOM.2024.178382

[16] J. H. Chen, et al. "Influence of interface on microstructure and mechanical properties of laser-direct energy deposited Ti60 alloy." Additive Manufacturing, vol.95, pp.104560-104560, 2024, https://doi.org/10.1016/J.ADDMA.2024.104560

[17] P. Li, et al. "Study on deformation behavior of Ti60 alloy based on multi-physics coupling." Materials Today Communications, vol.38, pp. 107931-, 2024, https://doi.org/10.1016/J.MTCOMM.2023.107931

[18] W. Z. Chen, et al. "The effect of NaCl-induced corrosion on Ti60's hot salt stress corrosion cracking." Corrosion Science, vol.226, 2024, https://doi.org/10.1016/J.CORSCI.2023.111677

[19] J.L. Pan, et al. "Study on HCF/VHCF properties and fatigue life prediction of Ti60 titanium alloy under three-point bending." International Journal of Fatigue, vol.209, pp. 109603-109603, 2026, https://doi.org/10.1016/J.IJFATIGUE.2026.109603

[20] R.X. He, et al. "Crack Initiation Mechanism and Life Prediction of Ti60 Titanium Alloy Considering Stress Ratios Effect in Very High Cycle Fatigue Regime." Materials, vol.15, no.8, pp. 2800-2800, 2022, https://doi.org/10.3390/MA15082800

 https://doi.org/10.64486/m.66.1.10